IMU In-Motion Alignment Without Benefit of Attitude Initialization

Dr. Robert M. Rogers
Rogers Engineering & Associates
Gainesville, FL 32605

BIOGRAPHY

Robert M. Rogers is sole proprietor performing research, systems analysis, test and evaluation for DoD and NASA. He received BS, MS and PhD degrees in Aerospace Engineering from the University of Florida, and is an Associate Fellow of the American Institute of Aeronautics and Astronautics (AIAA).

ABSTRACT

The problem addressed in this paper is the establishment of local level wander azimuth navigation and body reference frames for an Inertial Navigation System (INS) based on outputs of an Inertial Measurement Unit (IMU) without the use of initial attitude information. The availability of initial position and velocity in a geographic or earth centered reference frame is assumed. This information is consistent with that available from a Global Positioning System (GPS) receiver; however, in this paper an aircraft navigation systems' data is used instead. The formulation presented does not assume that the IMU's host vehicle heading and velocity are along the same direction. Alignment is accomplished using a Kalman filter algorithm implemented with an INS system error model formulated for large heading errors and using position measurement updates. This algorithm provides estimates of navigation frame referenced velocity, wander azimuth and body attitude errors that are used to continuously correct the on-going navigation solution calculations. The performance of the alignment algorithm is evaluated using actual IMU and aircraft data from flight tests.

INTRODUCTION

The problem of IMU alignment can be considered as being either an alignment transfer or an alignment without benefit of initial attitude information. An example of transfer alignment is the case in which the IMU's host vehicle (assuming a strap-down IMU) and a reference navigation system are initially coarsely aligned, and the reference navigation system's data to initialize the IMU's navigation equations. Since the IMU and reference navigation system are coarsely aligned, an INS system error model, based on small errors, can be used to improve upon the initialization and calibrate the IMU's errors [1].

Alignment without initial attitudes is normally the case for stationary ground alignment; however, the problem of in-motion alignment without initial attitudes is less frequently addressed. For an INS that has small errors, resulting from its initialization or having undergone some degree of alignment, the INS system error model is developed based on the assumption that the magnitudes of the error variables are small such that the products of these variables are negligible and only first order terms in these variables are retained in the error equations [2]. However, for an INS that is not aligned, larger errors occur which requires a reformulation of the error equations. This is the problem on in-motion alignment.

In-motion alignment INS error formulations utilize implementations of two azimuth angle error variables. Examples of these error variables are $\delta \sin(\alpha)$ & $\delta \cos(\alpha)$ [3] and [4] and $\delta \sin(\psi)$ & $\delta [1-\cos(\psi)]$ [5]. These formulations use the assumption that products of errors associated with these trigonometric functions and other error variables can again be neglected. In the following, the error equations are obtained using the first of the two azimuth angle error variables above to obtain a perturbation form of the INS error equations.

The data flow, for the in-motion alignment problem presented in this paper, is illustrated in Figure 1. Aircraft navigation system data is the source of initial position and velocity data referenced in a geographic frame. The alignment algorithm uses this latitude, ϕ, and longitude, λ, in the form of the geographic-to-earth direction cosine matrix, C_g^e, and altitude, h as measurement updates.

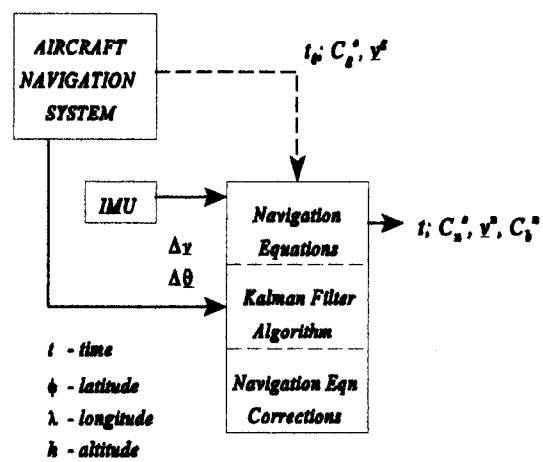

Figure 1: Aircraft, IMU and Navigation Data Flow

NAVIGATION EQUATIONS

The navigation equations are implemented as a local level wander azimuth system. The relationship between the local level geographic North-East-Down and wander azimuth frames is presented in Figure 2.

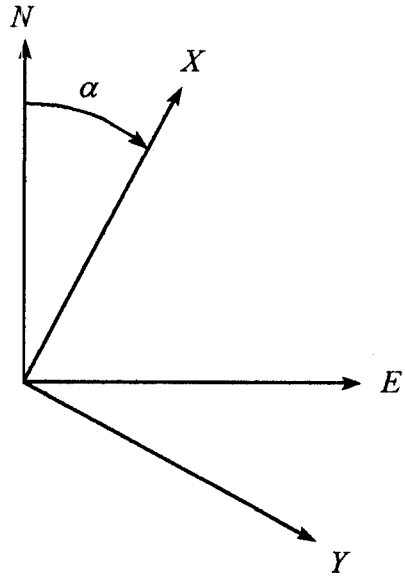

Figure 2: Local Level Geographic and Wander Azimuth Frames

The transformation from the geographic frame to the wander azimuth frame is give by the following matrix

$$C_g^{\ n} = \begin{bmatrix} \cos\alpha & \sin\alpha & 0 \\ -\sin\alpha & \cos\alpha & 0 \\ 0 & 0 & 1 \end{bmatrix} \tag{1}$$

Position

Position is maintained in the navigation-to-earth direction cosine matrix. This matrix, for the definition of the wander azimuth angle , α , given in Figure 2, is given as[1]

$$C_n^{\ e} = \begin{bmatrix} -c(\alpha)s(\phi)c(\lambda) - s(\alpha)s(\lambda) & s(\alpha)s(\phi)c(\lambda) - c(\alpha)s(\lambda) & -c(\phi)c(\lambda) \\ -c(\alpha)s(\phi)s(\lambda) + s(\alpha)c(\lambda) & s(\alpha)s(\phi)s(\lambda) + c(\alpha)c(\lambda) & -c(\phi)s(\lambda) \\ c(\alpha)c(\phi) & -s(\alpha)c(\phi) & -s(\phi) \end{bmatrix} \tag{2}$$

The evolution of this matrix is governed by the following homogeneous matrix differential equation

$$\dot{C}_e^{\ n} = -\Omega_{e/n}^n \, C_e^{\ n} \tag{3}$$

where $\Omega_{e/n}^n$ is the skew symmetric matrix equivalent of the vector cross product $(\underline{\omega}_{e/n}^n \ x)$. The vector is the rotation rate vector, from the navigation frame (wander azimuth) with respect to the earth centered earth fixed frame coordinatized in the navigation frame, and is also known as the transport rate.

[1] s() and c() represent sine() and cosine().

The transport rate vector $\underline{\omega}_{e/n}^n$ is expressed in terms of the wander azimuth frame velocities as

$$\underline{\omega}_{e/n}^n \equiv \underline{\rho} = \begin{bmatrix} \dfrac{v_y}{R_y} \\ -\dfrac{v_x}{R_x} \\ \rho_z \end{bmatrix} \tag{4}$$

The wander azimuth angle rate, in general, satisfies the following

$$\begin{aligned} \dot{\alpha} &= \dot{\lambda} \sin(\phi) + \rho_z \\ &= \frac{v_{east}}{(R_{normal}+h)} \tan(\phi) + \rho_z \\ &= -\rho_d + \rho_z \end{aligned} \tag{5}$$

where ρ_z & ρ_d are the last elements in the rotation vectors $\underline{\omega}_{e/n}^n$ and $\underline{\omega}_{e/g}^g$ respectively. Equation (5) can be shown by expanding the matrix elements in equation (3). The wander azimuth implementation requires

$$\rho_z \equiv 0 \tag{6}$$

Velocity

Velocity is obtained from the vector differential equation

$$\dot{\underline{v}}^n = \underline{f}^n - (\Omega_{e/n}^n + 2 \, \Omega_{i/e}^n) \, \underline{v}^n + \underline{g}^n \tag{7}$$

where

- $\underline{f}^n$ specific force vector in navigation frame (transformed from body referenced IMU's Δv outputs)
- $\Omega_{i/e}^n$ skew symmetric matrix equivalent of the vector cross product $(\underline{\omega}_{i/e}^n \ x)$, the rotation rate vector is from the earth centered earth fixed frame with respect to an inertial frame coordinatized in the navigation frame
- $\underline{g}^n$ gravity vector in navigation frame

The earth rotation vector $\underline{\omega}_{i/e}^n$ is expressed in wander azimuth frame components as

$$\underline{\omega}_{i/e}^n \equiv \underline{\Omega} = C_e^{\ n} \begin{bmatrix} 0 \\ 0 \\ \omega_{i/e} \end{bmatrix} \tag{8}$$

Attitude

Attitude is maintained in the body-to-navigation frame direction cosine matrix. This matrix is given as

$$C_b^n = \begin{bmatrix} c(\theta)c(\psi_{az}) & -c(\varphi)s(\psi_{az}) + s(\varphi)s(\theta)c(\psi_{az}) & s(\varphi)s(\psi_{az}) + c(\varphi)s(\theta)c(\psi_{az}) \\ c(\theta)s(\psi_{az}) & c(\varphi)c(\psi_{az}) + s(\varphi)s(\theta)s(\psi_{az}) & -s(\varphi)c(\psi_{az}) + c(\varphi)s(\theta)s(\psi_{az}) \\ -s(\theta) & s(\varphi)c(\theta) & c(\varphi)c(\theta) \end{bmatrix} \tag{9}$$

where ψ_{az} is related to wander azimuth and true heading by

$$\psi_T = \alpha + \psi_{az} \tag{10}$$

The evolution of the C_b^n matrix is governed by the following matrix differential equation

$$\dot{C}_n^b = -\Omega_{n/b}^b \, C_n^b \tag{11}$$

where, using the angular velocity addition theorem, the angular rotation matrix $\Omega_{n/b}^b$ is obtained from the elements of the following angle rate vector

$$\underline{\omega}_{n/b}^b = -C_n^b \left(\underline{\omega}_{e/n}^n + \underline{\omega}_{i/e}^n \right) + \underline{\omega}_{i/b}^b \tag{12}$$

where the last term represents the IMU's $\Delta\theta$ outputs.

Navigation Equation Initialization

Equations (3), (7) and (11) require initialization before they can be integrated. This is the primary problem for in-motion alignment. Since it is assumed that position - latitude and longitude - are known, some of the terms of the matrix in equation (2) can be computed; however, the wander azimuth angle is unknown. Since the wander azimuth angle is unknown, the available initial geographic frame velocity components cannot be transformed into the corresponding initial values for the wander azimuth frame components. It is also assumed that the initial attitudes, *roll* - φ, *pitch* - θ, & ψ_{az}, are unknown. As a result, none of the terms for the elements of the matrix in equation (9) can be computed.

To address these apparent limitations, the following assumptions are made. Proceeding in the reverse order, it is assumed that the initial attitudes are all zero. This assumption produces an identity matrix for the initial value of the C_b^n matrix for equation (11). Even though there is a likelihood of large wander azimuth angles, up to 180 degrees, the initial wander azimuth angle is assumed to be zero in equation (1), and the geographic frame initial velocities are transformed into the wander azimuth frame. The elements in equation (2) are also computed with zero wander azimuth angle.

With these assumptions, the equations (3), (7) and (11) are initialized and integrated. However, the resulting navigation solution will have significant errors. It is the task of the alignment algorithm to provide estimates of the wander angle and attitude errors that are then used to correct the ongoing integration of the navigation equations. Since the wander azimuth errors are large during this process, this is referred to as "Coarse Alignment".

ALIGNMENT SYSTEM ERROR EQUATIONS

System Error Dynamics

Large Azimuth Error Model

Presented in Appendix A is the development of the INS system error dynamics for large azimuth errors associated with the coarse alignment. This development proceeds with the C_e^n matrix is factored into the following product

$$C_e^n = C_g^n \, C_e^g \tag{13}$$

The computed $\overline{C}_e^n$ matrix is represented and expanded in terms of each matrix's errors as

$$\begin{aligned} \overline{C}_e^n &= \overline{C}_g^n \, \overline{C}_e^g \\ &= \left(C_g^n + \delta C_g^n \right) \left[I - (\delta\underline{\theta}^g \, x) \right] C_e^g \end{aligned} \tag{14}$$

This representation yields the following C_e^n error matrix

$$\begin{aligned} \delta C_e^n &= \overline{C}_e^n - C_e^n \\ &= E \, C_n^g \, C_e^n \end{aligned} \tag{15}$$

Therefore, position error is obtained from the E error matrix

$$E \equiv \begin{bmatrix} \delta\, c\alpha & \delta\, s\alpha & -\delta\theta_y \\ -\delta\, s\alpha & \delta\, c\alpha & \delta\theta_x \\ \delta\theta_e & -\delta\theta_n & 0 \end{bmatrix} \tag{16}$$

Error in the wander azimuth angle is incorporated as error in the trigonometric sine and cosine functions - $\delta\, s\alpha$ & $\delta\, c\alpha$ - respectively. It is shown in Appendix A that this matrix is governed by the following matrix differential equation

$$\dot{E} = E \, \Omega_{e/g}^g - \Omega_{e/n}^n \, E + \left(\Omega_{e/n}^n - \overline{\Omega}_{e/n}^n \right) C_g^n \tag{17}$$

From the developments in Appendix A, the following correspondence exists between the *small azimuth* error, defined in the small angle perturbation forms of the INS system error models [2], and the *large azimuth* error matrix in equation (16):

$$-(\delta\underline{\theta} \, x) \sim E \, C_n^g \tag{18}$$

This correspondence is used to obtain the velocity and attitude error equations from the small angle perturbation forms of the INS system error dynamic equations. The resulting INS system error dynamics, for coarse alignment, is summarized in Figure 3. During the coarse alignment, it is assumed that the errors in the trigonometric functions $\delta\, s\alpha$ & $\delta\, c\alpha$ are constant and that the z-axis tilt error is zero - $\phi_z = 0$.

Small Azimuth Error Model

The perturbation form of INS system error dynamics for the fine alignment can be obtained by using the following equations

$$\delta\, s\alpha = c\alpha \, \delta\alpha \tag{19}$$

$$\delta\, c\alpha = -s\alpha \, \delta\alpha \tag{20}$$

It is shown in Appendix B that the large azimuth INS system error dynamics in Figure 3 collapse to that in Figure 4.

$$\frac{d}{dt}\begin{bmatrix} \delta\theta_x \\ \delta\theta_y \\ \delta h \\ \delta v_x^n \\ \delta v_y^n \\ \delta v_z^n \\ \phi_x \\ \phi_y \\ \delta\, s\alpha \\ \delta\, c\alpha \end{bmatrix} = \begin{bmatrix} 0 & 0 & -\frac{v_y}{R^2} & 0 & \frac{1}{R} & 0 & 0 & 0 & -\rho_e & -\rho_n \\ 0 & 0 & \frac{v_x}{R^2} & -\frac{1}{R} & 0 & 0 & 0 & 0 & \rho_n & -\rho_e \\ 0 & 0 & 0 & 0 & 0 & -1 & 0 & 0 & 0 & 0 \\ -(v_y\Omega_y + 2v_z\Omega_z) & v_y\Omega_x & -\frac{v_x v_z}{R^2} & \frac{v_z}{R} & 2\Omega_z & -(\rho+2\Omega)_y & -v_y\omega_y & (v_y\omega_x - f_z) & 2v_z\Omega_n & 0 \\ v_x\Omega_y & -(v_x\Omega_x + 2v_z\Omega_z) & -\frac{v_y v_z}{R^2} & -2\Omega_z & \frac{v_z}{R} & (\rho+2\Omega)_x & (v_x\omega_y + f_z) & -v_x\omega_x & 0 & 2v_z\Omega_n \\ 2v_x\Omega_z & 2v_y\Omega_z & \frac{v_x^2+v_y^2}{R^2} & 2(\rho+\Omega)_y & -2(\rho+\Omega)_x & 0 & -f_y & f_x & -2v_x\Omega_n & -2v_y\Omega_n \\ 0 & -\Omega_z & -\frac{v_y}{R^2} & 0 & \frac{1}{R} & 0 & 0 & \Omega_z & 0 & \Omega_n \\ \Omega_z & 0 & \frac{v_x}{R^2} & -\frac{1}{R} & 0 & 0 & -\Omega_z & 0 & -\Omega_n & 0 \\ 0 & 0 & 0 & 0 & 0 & 0 & 0 & 0 & 0 & 0 \\ 0 & 0 & 0 & 0 & 0 & 0 & 0 & 0 & 0 & 0 \end{bmatrix} \begin{bmatrix} \delta\theta_x \\ \delta\theta_y \\ \delta h \\ \delta v_x^n \\ \delta v_y^n \\ \delta v_z^n \\ \phi_x \\ \phi_y \\ \delta\, s\alpha \\ \delta\, c\alpha \end{bmatrix}$$

$$+ \begin{bmatrix} 0 \\ 0 \\ 0 \\ -v_y\ \epsilon_z \\ v_x\ \epsilon_z \\ 0 \\ 0 \\ 0 \\ 0 \\ 0 \end{bmatrix} + \begin{bmatrix} 0 \\ 0 \\ 0 \\ \delta f_x \\ \delta f_y \\ \delta f_z \\ 0 \\ 0 \\ 0 \\ 0 \end{bmatrix} + \begin{bmatrix} 0 \\ 0 \\ 0 \\ \delta g_x \\ \delta g_y \\ \delta g_z \\ 0 \\ 0 \\ 0 \\ 0 \end{bmatrix} + \begin{bmatrix} 0 \\ 0 \\ 0 \\ 0 \\ 0 \\ 0 \\ \epsilon_x \\ \epsilon_y \\ 0 \\ 0 \end{bmatrix}$$

Figure 3: INS Coarse Alignment System Error Dynamics

$$\frac{d}{dt}\begin{bmatrix} \delta\theta_x \\ \delta\theta_y \\ \delta h \\ \delta v_x^n \\ \delta v_y^n \\ \delta v_z^n \\ \phi_x \\ \phi_y \\ -(\delta\alpha) \end{bmatrix} = \begin{bmatrix} 0 & 0 & -\frac{v_y}{R^2} & 0 & \frac{1}{R} & 0 & 0 & 0 & \rho_y \\ 0 & 0 & \frac{v_x}{R^2} & -\frac{1}{R} & 0 & 0 & 0 & 0 & -\rho_x \\ 0 & 0 & 0 & 0 & 0 & -1 & 0 & 0 & 0 \\ -(v_y\Omega_y + 2v_z\Omega_z) & v_y\Omega_x & -\frac{v_x v_z}{R^2} & \frac{v_z}{R} & 2\Omega_z & -(\rho+2\Omega)_y & -v_y\omega_y & (v_y\omega_x - f_z) & -2v_z\Omega_x \\ v_x\Omega_y & -(v_x\Omega_x + 2v_z\Omega_z) & -\frac{v_y v_z}{R^2} & -2\Omega_z & \frac{v_z}{R} & (\rho+2\Omega)_x & (v_x\omega_y + f_z) & -v_x\omega_x & -2v_z\Omega_y \\ 2v_x\Omega_z & 2v_y\Omega_z & \frac{v_x^2+v_y^2}{R^2} & 2(\rho+\Omega)_y & -2(\rho+\Omega)_x & 0 & -f_y & f_x & 2(v_x\Omega_x + v_y\Omega_y) \\ 0 & -\Omega_z & -\frac{v_y}{R^2} & 0 & \frac{1}{R} & 0 & 0 & \Omega_z & -\Omega_y \\ \Omega_z & 0 & \frac{v_x}{R^2} & -\frac{1}{R} & 0 & 0 & -\Omega_z & 0 & \Omega_x \\ -\omega_y & \omega_x & 0 & 0 & 0 & 0 & \omega_y & -\omega_x & 0 \end{bmatrix} \begin{bmatrix} \delta\theta_x \\ \delta\theta_y \\ \delta h \\ \delta v_x^n \\ \delta v_y^n \\ \delta v_z^n \\ \phi_x \\ \phi_y \\ -(\delta\alpha) \end{bmatrix}$$

$$+ \begin{bmatrix} 0 \\ 0 \\ 0 \\ -v_y\ \epsilon_z \\ v_x\ \epsilon_z \\ 0 \\ 0 \\ 0 \\ 0 \end{bmatrix} + \begin{bmatrix} 0 \\ 0 \\ 0 \\ \delta f_x \\ \delta f_y \\ \delta f_z \\ 0 \\ 0 \\ 0 \end{bmatrix} + \begin{bmatrix} 0 \\ 0 \\ 0 \\ \delta g_x \\ \delta g_y \\ \delta g_z \\ 0 \\ 0 \\ 0 \end{bmatrix} + \begin{bmatrix} 0 \\ 0 \\ 0 \\ 0 \\ 0 \\ 0 \\ \epsilon_x \\ \epsilon_y \\ \epsilon_z \end{bmatrix}$$

Figure 4: INS Fine Alignment System Error Dynamics

Observations

The coarse and fine alignment filter's system error dynamic models, summarized in Figures 3 and 4 respectively, incorporate angular position error states referenced in the wander azimuth frame. The measurements are formed to be consistent with these system error dynamic models. In the following, it is assumed that positions, from an independent reference source are available. These positions can be in the form of latitudes, longitudes and altitudes from either an aircraft navigation system or GPS receiver. An approach similar to that presented below can also use earth centered earth fixed referenced positions to form the measurements.

Consider again the C_n^e in equation (2). Each of the columns of this matrix are orthogonal unit vectors. A third column unit vector, formed from the aircraft navigation system's latitude and longitude can be expressed as

$$\underline{t}_3 \equiv \begin{bmatrix} C_{n\,13}^{e} \\ C_{n\,23}^{e} \\ C_{n\,33}^{e} \end{bmatrix} \tag{21}$$

First and second column vectors, formed from the INS navigation solution's computed $\overline{C}_n^e$ matrix, are

$$\underline{\bar{s}}_1 \equiv \begin{bmatrix} \overline{C}_{n\,11}^{e} \\ \overline{C}_{n\,21}^{e} \\ \overline{C}_{n\,31}^{e} \end{bmatrix} \quad \& \quad \underline{\bar{s}}_2 \equiv \begin{bmatrix} \overline{C}_{n\,12}^{e} \\ \overline{C}_{n\,22}^{e} \\ \overline{C}_{n\,32}^{e} \end{bmatrix} \tag{22}$$

The following vector dot products yield the differences in the wander azimuth frame referenced angular position vectors:

$$\Delta\theta_x = \underline{\bar{s}}_2 \cdot \underline{t}_3 \tag{23}$$

$$\Delta\theta_y = -\underline{\bar{s}}_1 \cdot \underline{t}_3 \tag{24}$$

These results can be shown by expanding the computed $\overline{C}_n^e$ matrix in terms of the true latitude, longitude and wander angle values plus their corresponding perturbation error variables (see the next section); performing the indicated product; and finally collecting terms of first order in the latitude, longitude and wander angle perturbation error variables. The latitude and longitude perturbation error variable terms can be shown to correspond to the associated wander azimuth frame angular position errors as outlined in the next section.

The wander azimuth frame angular position error differences above suggests the following measurement matrix/state vector product

$$H\,\underline{x} = \begin{bmatrix} 1 & 0 & 0 & \cdots \\ 0 & 1 & 0 & \cdots \\ 0 & 0 & 1 & \cdots \end{bmatrix} \begin{bmatrix} \delta\theta_x \\ \delta\theta_y \\ \delta h \\ \vdots \end{bmatrix} \tag{25}$$

ALIGNMENT FILTER CORRECTIONS

The alignment filter algorithm implements the system error models summarized in Figures 3 and 4. Estimates from these algorithms are used to correct the navigation equations. These corrections are in the form of position, velocity, attitude, and inertial instrument errors of accelerometer and gyro biases.

Position Corrections

The position (latitude, longitude and wander azimuth) is maintained by the C_n^e matrix given in equation (2). If the error in the computed $\overline{C}_n^e$ matrix is represented by

$$\overline{C}_e^{\,n} = [\, I - (\delta\underline{\theta}\, x) \,]\, C_e^{\,n} \tag{26}$$

using the following representations for error in the computed latitude, longitude and wander azimuth angles (assuming small error angles)

$$\overline{\phi} = \phi + \delta\phi \tag{27}$$

$$\overline{\lambda} = \lambda + \delta\lambda \tag{28}$$

and

$$\overline{\alpha} = \alpha + \delta\alpha \tag{29}$$

and equating the computed $\overline{C}_n^e$ matrix, expressed in terms of its computed latitude, longitude and wander azimuth angles above, to the error form indicated in equation (26), yields the following expressions for latitude and longitude errors

$$\delta\phi = -s\alpha\ \delta\theta_x - c\alpha\ \delta\theta_y \tag{30}$$

and

$$\delta\lambda = \frac{c\alpha\ \delta\theta_x - s\alpha\ \delta\theta_y}{c\phi} \tag{31}$$

During coarse alignment, the wander azimuth error , $\delta\alpha$, for the navigation solution corrections is obtained from the algorithm's states and expressions for $\delta\, s\alpha$ & $\delta\, c\alpha$ given in equations (19) and (20). This error correction is obtained from the following product of the system state elements as

$$\begin{aligned} c\alpha\ \delta\, s\alpha - s\alpha\ \delta\, c\alpha &= c\alpha\ (c\alpha\ \delta\alpha) - s\alpha\ (-s\alpha\ \delta\alpha) \\ &= (s^2\alpha + c^2\alpha)\ \delta\alpha \end{aligned} \tag{32}$$

Or

$$\delta\alpha = c\alpha\ \delta\, s\alpha - s\alpha\ \delta\, c\alpha \tag{33}$$

For fine alignment, the wander azimuth error is obtained directly from the alignment algorithm's $\delta\alpha$ state.

Equations (30) and (31) and either equation (33) during coarse alignment or the $\delta\alpha$ system state during fine alignment, are used to correct the computed latitude, longitude and wander azimuth angles by subtracting the values of these variables, formed from the alignment filter's states, from the computed values (the reverse of equations (27), (28) and (29)). The corrected C_n^e matrix, given in equation (2), is re-computed based on these corrections.

Velocity Corrections

The velocity errors are represented, in the perturbation form, by

$$\bar{\underline{v}}^n = \underline{v}^n + \delta\underline{v}^n \tag{34}$$

The reverse of this equation is used to apply the corrections from the coarse alignment filter's estimates.

Attitude Corrections

Attitude is maintained by the C_b^n matrix in equation (9). The error in the computed $\bar{C}_b^n$ matrix is represented as

$$\bar{C}_b^n = [\, I - (\underline{\Phi}\, x) \,]\, C_b^n \tag{35}$$

During alignment, the z-axis component of the tilt error vector assumed to be zero. Therefore, the attitude corrections are applied using the reverse of this equation with $\phi_z = 0$.

IN-MOTION ALIGNMENT RESULTS

Flight test data is used for the results presented in this paper. This data was obtained during the recently completed U.S. Air Force EDGE (Exploitation of Differential GPS Enhancement) program. The data used for this paper from this program includes the aircraft's navigation system data and weapon IMU output data as illustrated in Figure 1. This data was also used in a previous evaluation of transfer alignment [1]. The results presented in the following uses data from Pass #4 (see [1]) of the captive carry flight tests. During the EDGE captive tests, a sequence of maneuvers were executed to accomplish the transfer alignment of the EDGE test vehicle's IMU and to line the aircraft up for a simulated release of the test vehicle. After this simulated release point, the aircraft was maneuvered such that it's trajectory followed a typical free-flight trajectory of the test vehicle.

The navigation solution's C_n^e matrix, given in equation (2), is initialized with the aircraft's latitude and longitude, and wander angle is initialized to zero. The attitude initialization for the C_b^n matrix, given in equation (9), assumes zero for *roll*, *pitch* & ψ_{az}. The integrated outputs from the navigation equations are processed initially in the coarse alignment algorithm, then, after some error reduction, in the fine alignment algorithm. Estimates provided by the alignment algorithms are used to correct the on-going navigation solution variables for subsequent integration between the algorithm's updates.

Presented in the following are results using the coarse alignment filter by itself, whose INS dynamic error model is presented in Figure 3, and a combined coarse and fine alignment filter, whose fine alignment INS dynamic error model is presented in Figure 4. The transition from coarse alignment to fine alignment based on the magnitude of the estimation uncertainty associated with the wander azimuth error obtained in equation (33).

Shown in Figure 5 is the flight profile flown for the Pass #4 captive carry test data used for the results presented. Included in this figure are the aircraft navigation system's (F16) and the computed navigation solution's (INS) positions. The computed navigation solution shown in this figure is based on using only the coarse alignment algorithm's corrections to the navigation solution without the transition to the fine alignment algorithm The aircraft is initially near 30.6° latitude and -86.7° longitude with an initial true heading of approximately 60° from north. There is an initial straight flight segment with an approximate 30 degree right turn heading change towards the east, followed by an approximate 210 degree right turn heading change towards the west, followed by an approximate 70 degree left turn heading change towards the southwest.

Subsequent figures illustrate the benefit of a transition from the coarse alignment to fine alignment filter models. This transition is based on the coarse alignment filter's estimation uncertainty of the wander azimuth error and occurs for this data set at approximately 46850 seconds. Shown in Figure 6 are: INS computed azimuths {INS wander angle (INS_WA), INS azimuth (INS_PSIaz), and INS true heading (INS_TRUE w/TRN) using the coarse alignment with transition to fine alignment}; INS true heading (INS_TRUE-CRS) {using only the coarse alignment filter}; and F16 true heading (F16_TRUE). From its zero value initialization, the INS computed true heading is relatively unchanged until the initial right turn heading change. With this heading change, the INS computed true heading approaches the F16 true heading - a change of greater than 60 degrees. During the second right turn, convergence to the F16 true heading is completed.

Shown in Figure 7 are the computed INS true heading (INS_TRUE) results for the initial right turn heading change from Figure 6 with an expanded plot scale. The comparison between the combined coarse with transition to fine alignment filters' results with those using only the coarse alignment filter shows a more rapid convergence to the F16's true heading during the second right turn for the combined filters.

The EDGE captive carry tests simulated a test vehicle free-flight near the end of the flight profile. For this time period, the alignment (filter measurement updates) are suspended allow for an evaluation of the unaided navigation system errors and thus the quality of the alignment achieved. The alignment is suspended at approximately 47165 seconds for both the combined coarse with transition to fine alignment filter and the coarse alignment filter only. Figure 8 presents results from Figure 6 expanded for this simulated free-flight portion of this EDGE test data segment. Presented for comparison are the computed INS true heading for the combined coarse with transition to fine alignment filters' results and the results using only the coarse alignment filter. These results show that the combined filter results continue to be in more close agreement with the F16 true heading than the results with only the coarse alignment filter after the alignment is suspended. These results show the benefit of transitioning to the fine alignment form of INS system error dynamic model by providing better attitudes.

Shown in Figures 9 and 10 are position errors, $-\delta\theta_y * R$ & $\delta\theta_x * R$, for the combined filters and the coarse alignment filter respectively for the entire captive test segment. Also presented in these figures are aircraft's pitch and roll scaled fit onto the

same plot. These transient errors are an indication of the degree of completeness of the alignment for both the combined alignment filters and the coarse alignment filter. Large transients in the position errors occur during the initial heading change seen in Figure 5. Smaller transients during later maneuvers are the result of improvements to the navigation solution based on the alignment filter(s) corrections. In both figures, after the second right turn heading change, the position errors remain small until the simulated free-flight time point at which the alignment process is suspended. After this time, navigation solution is no longer corrected. An examination of these two figures shows a much larger position error growth after the alignment is suspended for results from using only the coarse alignment filter. These results show the benefit, in terms of a relative performance improvement, of transitioning to the fine alignment form of the INS system error dynamic model by providing improved free-inertial navigation performance.

The flight test profile and resulting data used to present the results of the in-motion alignment were not designed with the purpose of accomplishing an in-motion alignment but a transfer alignment. Had in-motion alignment been considered, a different profile, allowing more settling time between maneuvers, may have yielded better results.

SUMMARY

In this paper, coarse and fine alignment filter INS system error dynamic models for a local level wander azimuth navigation system has been developed. The coarse alignment filter implements an INS system error dynamic model formulated for large heading errors. Using actual flight test data for the IMU and aircraft navigation positions, the ability of this alignment filter to estimate large errors in attitudes has been demonstrated, this without benefit of attitude initialization of the navigation equations. Transitioning to a small angle error filter for fine alignment, further improved the alignment results.

REFERENCES

[1] Rogers, R.M., "Weapon IMU Transfer Alignment Using Aircraft Position from Actual Flight Tests," IEEE Position, Location and Navigation Symposium, 1996.

[2] Rogers, R.M., "Velocity Error Representations in Inertial Navigation System Error Models", AIAA Guidance, Navigation and Control Conference, 1995.

[3] Kelly, R.T, et al, "Design, Development & Evaluation of an ADA Coded INS/GPS Open Loop Kalman Filter", IEEE National Aerospace Electronics Conference, 1990.

[4] Pham, T.M., "Kalman Filter Mechanization for INS Airstart", IEEE AES Systems Magazine, January 1992.

[5] Scherzinger, B.M., "Inertial Navigation Error Models for Large Heading Uncertainty", IEEE Position, Location and Navigation Symposium, 1996.

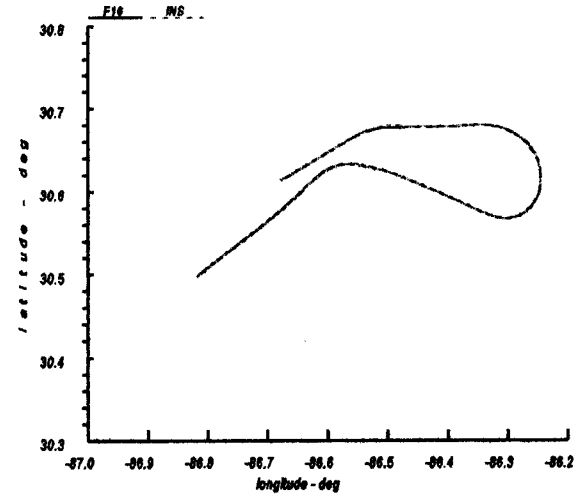

Figure 5: F-16 and INS Positions for Coarse Alignment

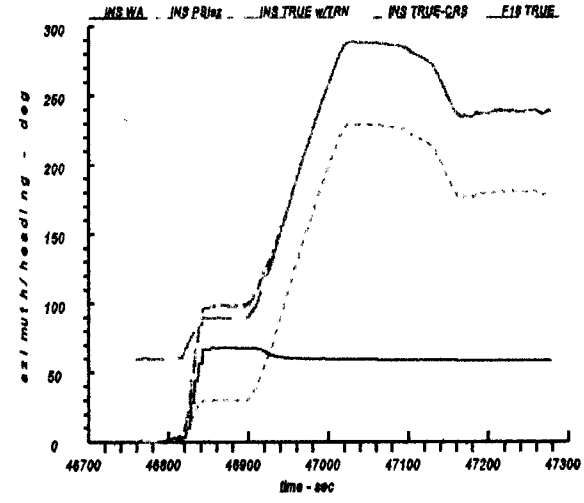

Figure 6: INS and F16 True Heading for Combined & Coarse Alignments

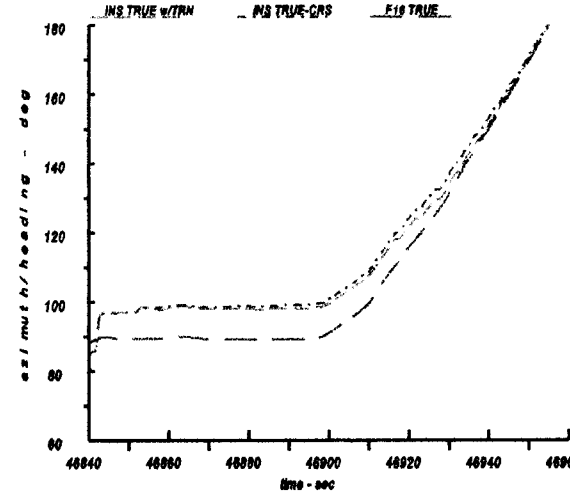

Figure 7: True Headings during Initial Heading Change

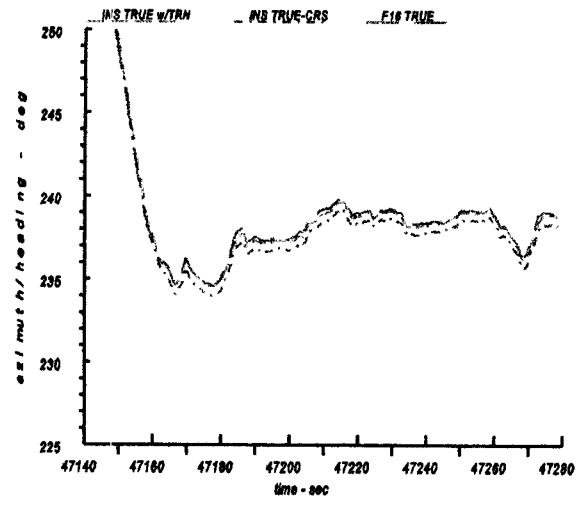

Figure 8: True Headings for Suspended Alignments

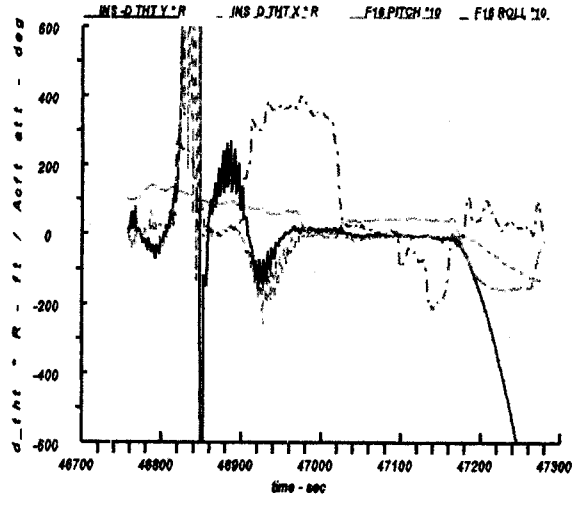

Figure 9: Position Errors for Coarse Alignment

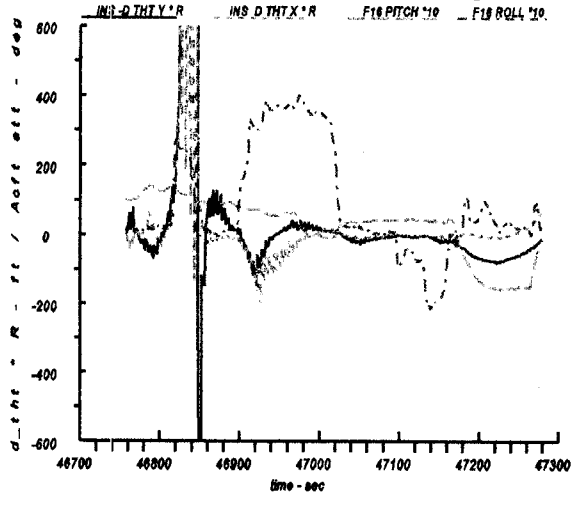

Figure 10: Position Errors for Combined Coarse & Fine Alignment w/Transition

APPENDIX A

Coarse Alignment Error Equations

The process of alignment is to establish the wander azimuth angle For the transformation from earth-to-navigation frame - C_e^n - and for the transformation from body-to-navigation frame - C_b^n - , the final transformation arriving at the navigation frame is an azimuth rotation. In the following, it is assumed that the error associated with the C_b^n azimuth rotation, the z-tilt error, is zero - $\phi_z \equiv 0$ - and all azimuth error is attributed to the wander azimuth angle.

Position Error Equations

Proceeding from equation (14), this expression is further expanded to represent errors in north and east position, angular position errors, and errors in the sinα & cosα terms

$$\overline{C}_e^n = \left(\begin{bmatrix} c\alpha & s\alpha & 0 \\ -s\alpha & c\alpha & 0 \\ 0 & 0 & 1 \end{bmatrix} + \begin{bmatrix} \delta c\alpha & \delta s\alpha & 0 \\ -\delta s\alpha & \delta c\alpha & 0 \\ 0 & 0 & 0 \end{bmatrix} \right) \begin{bmatrix} 1 & 0 & -\delta\theta_e \\ 0 & 1 & \delta\theta_n \\ \delta\theta_e & -\delta\theta_n & 1 \end{bmatrix} C_e^g$$

$$\approx C_g^n \begin{bmatrix} 1 & 0 & -\delta\theta_e \\ 0 & 1 & \delta\theta_n \\ \delta\theta_e & -\delta\theta_n & 1 \end{bmatrix} C_n^g C_e^n + \begin{bmatrix} \delta c\alpha & \delta s\alpha & 0 \\ -\delta s\alpha & \delta c\alpha & 0 \\ 0 & 0 & 0 \end{bmatrix} C_n^g C_e^n$$

$$= C_e^n + C_g^n \begin{bmatrix} 0 & 0 & -\delta\theta_e \\ 0 & 0 & \delta\theta_n \\ \delta\theta_e & -\delta\theta_n & 0 \end{bmatrix} C_n^g C_e^n + \begin{bmatrix} \delta c\alpha & \delta s\alpha & 0 \\ -\delta s\alpha & \delta c\alpha & 0 \\ 0 & 0 & 0 \end{bmatrix} C_n^g C_e^n$$

$$= C_e^n + \begin{bmatrix} 0 & 0 & -\delta\theta_y \\ 0 & 0 & \delta\theta_x \\ \delta\theta_e & -\delta\theta_n & 0 \end{bmatrix} C_n^g C_e^n + \begin{bmatrix} \delta c\alpha & \delta s\alpha & 0 \\ -\delta s\alpha & \delta c\alpha & 0 \\ 0 & 0 & 0 \end{bmatrix} C_n^g C_e^n$$

$$= C_e^n + \begin{bmatrix} \delta c\alpha & \delta s\alpha & -\delta\theta_y \\ -\delta s\alpha & \delta c\alpha & \delta\theta_x \\ \delta\theta_e & -\delta\theta_n & 0 \end{bmatrix} C_n^g C_e^n$$

$$\equiv (I + E\, C_n^g)\, C_e^n \qquad \text{A-1}$$

where the following have been used in between the fourth and fifth steps in equation A-1

$$\delta\theta_x = c\alpha\, \delta\theta_n + s\alpha\, \delta\theta_e \qquad \text{A-2}$$

$$\delta\theta_y = -s\alpha\, \delta\theta_n + c\alpha\, \delta\theta_e \qquad \text{A-3}$$

Position Error Dynamics

The position error dynamic equations, time derivative expressions for the angular position errors $\delta\theta_x$ & $\delta\theta_y$, for the coarse alignment with the $\delta s\alpha$ & $\delta c\alpha$ states are obtained in a similar manner as were those for the small perturbation angles. However, since the error representation is not in a convenient vector form (see equation (16)), each component must be evaluated rather using generalized vector algebra.

First consider the direction cosine matrix error

$$\delta C_e^n = \bar{C}_e^n - C_e^n \approx E\, C_e^g \tag{A-4}$$

The derivative of the second row of this equation is

$$\begin{aligned}\dot{\delta C}_e^n &= \dot{E}\, C_e^g + E\, \dot{C}_e^g \\ &= \dot{E}\, C_e^g - E\, \Omega_{e/g}^g\, C_e^g \\ &= (\dot{E} - E\, \Omega_{e/g}^g)\, C_e^g\end{aligned} \tag{A-5}$$

where

$$\dot{C}_e^g = -\Omega_{e/g}^g\, C_e^g \tag{A-6}$$

and $\Omega_{e/g}^g$ is used notationally to represent the skew symmetric equivalent of the vector cross product $-(\underline{\omega}_{e/g}^g \times)$.

Returning to the first row in equation A-4 and taking the derivative yields

$$\begin{aligned}\dot{\delta C}_e^n &= \dot{\bar{C}}_e^n - \dot{C}_e^n \\ &= -\bar{\Omega}_{e/n}^n\, \bar{C}_e^n + \Omega_{e/n}^n\, C_e^n \\ &= -\bar{\Omega}_{e/n}^n\, \bar{C}_g^n\, \bar{C}_e^g + \Omega_{e/n}^n\, C_g^n\, C_e^g \\ &= -\bar{\Omega}_{e/n}^n \left(C_g^n + \begin{bmatrix} \delta c\alpha & \delta s\alpha & 0 \\ -\delta s\alpha & \delta c\alpha & 0 \\ 0 & 0 & 0 \end{bmatrix} \right) \begin{bmatrix} 1 & 0 & -\delta\theta_e \\ 0 & 1 & \delta\theta_n \\ \delta\theta_e & -\delta\theta_n & 1 \end{bmatrix} C_e^g + \Omega_{e/n}^n C_g^n C_e^g \\ &= \left(-\bar{\Omega}_{e/n}^n \left(C_g^n + \begin{bmatrix} \delta c\alpha & \delta s\alpha & 0 \\ -\delta s\alpha & \delta c\alpha & 0 \\ 0 & 0 & 0 \end{bmatrix} \right) \begin{bmatrix} 1 & 0 & -\delta\theta_e \\ 0 & 1 & \delta\theta_n \\ \delta\theta_e & -\delta\theta_n & 1 \end{bmatrix} + \Omega_{e/n}^n C_g^n \right) C_e^g\end{aligned}$$

Equating equations A-5 and A-7

$$\begin{aligned}\dot{E} - E\, \Omega_{e/g}^g &= -\bar{\Omega}_{e/n}^n \left(C_g^n + \begin{bmatrix} \delta c\alpha & \delta s\alpha & 0 \\ -\delta s\alpha & \delta c\alpha & 0 \\ 0 & 0 & 0 \end{bmatrix} \right) \begin{bmatrix} 1 & 0 & -\delta\theta_e \\ 0 & 1 & \delta\theta_n \\ \delta\theta_e & -\delta\theta_n & 1 \end{bmatrix} + \Omega_{e/n}^n C_g^n \\ &\approx -\bar{\Omega}_{e/n}^n C_g^n - \bar{\Omega}_{e/n}^n \begin{bmatrix} \delta c\alpha & \delta s\alpha & 0 \\ -\delta s\alpha & \delta c\alpha & 0 \\ 0 & 0 & 0 \end{bmatrix} - \bar{\Omega}_{e/n}^n C_g^n \begin{bmatrix} 0 & 0 & -\delta\theta_e \\ 0 & 0 & \delta\theta_n \\ \delta\theta_e & -\delta\theta_n & 0 \end{bmatrix} + \Omega_{e/n}^n C_g^n \\ &\approx (\Omega_{e/n}^n - \bar{\Omega}_{e/n}^n) C_g^n - \bar{\Omega}_{e/n}^n \left(\begin{bmatrix} \delta c\alpha & \delta s\alpha & 0 \\ -\delta s\alpha & \delta c\alpha & 0 \\ 0 & 0 & 0 \end{bmatrix} + C_g^n \begin{bmatrix} 0 & 0 & -\delta\theta_e \\ 0 & 0 & \delta\theta_n \\ \delta\theta_e & -\delta\theta_n & 0 \end{bmatrix} \right) \\ &= (\Omega_{e/n}^n - \bar{\Omega}_{e/n}^n)\, C_g^n - \Omega_{e/n}^n \begin{bmatrix} \delta c\alpha & \delta s\alpha & -\delta\theta_y \\ -\delta s\alpha & \delta c\alpha & \delta\theta_x \\ \delta\theta_e & -\delta\theta_n & 0 \end{bmatrix}\end{aligned}$$

Or,

$$\dot{E} = E\, \Omega_{e/g}^g - \Omega_{e/n}^n E + (\Omega_{e/n}^n - \bar{\Omega}_{e/n}^n)\, C_g^n \tag{17}$$

In this equation, the terms of interest are in the third column - first and second row - of the E matrix.

Expanding each term in this equation

$$E\, \Omega_{e/g}^g = \begin{bmatrix} \delta c\alpha & \delta s\alpha & -\delta\theta_y \\ -\delta s\alpha & \delta c\alpha & \delta\theta_x \\ \delta\theta_e & -\delta\theta_n & 0 \end{bmatrix} \begin{bmatrix} 0 & -\rho_d & \rho_e \\ \rho_d & 0 & -\rho_n \\ -\rho_e & \rho_n & 0 \end{bmatrix}$$

$$= \begin{bmatrix} \delta s\alpha\, \rho_d + \delta\theta_y\, \rho_e & -\delta c\alpha\, \rho_d - \delta\theta_y\, \rho_n & \delta c\alpha\, \rho_e - \delta s\alpha\, \rho_n \\ \delta c\alpha\, \rho_d - \delta\theta_x\, \rho_e & \delta s\alpha\, \rho_d + \delta\theta_x\, \rho_n & -\delta s\alpha\, \rho_e - \delta c\alpha\, \rho_n \\ -\delta\theta_n\, \rho_d & -\delta\theta_e\, \rho_d & \delta\theta_e\, \rho_e + \delta\theta_n\, \rho_n \end{bmatrix} \tag{A-9}$$

$$\Omega_{e/n}^n E = \begin{bmatrix} 0 & -\rho_z & \rho_y \\ \rho_z & 0 & -\rho_x \\ -\rho_y & \rho_x & 0 \end{bmatrix} \begin{bmatrix} \delta c\alpha & \delta s\alpha & -\delta\theta_y \\ -\delta s\alpha & \delta c\alpha & \delta\theta_x \\ \delta\theta_e & -\delta\theta_n & 0 \end{bmatrix}$$

$$= \begin{bmatrix} \rho_z\, \delta s\alpha + \rho_y\, \delta\theta_e & -\rho_z\, \delta c\alpha - \rho_y\, \delta\theta_n & -\rho_z\, \delta\theta_x \\ \rho_z\, \delta c\alpha - \rho_x\, \delta\theta_e & \rho_z\, \delta s\alpha + \rho_x\, \delta\theta_n & -\rho_z\, \delta\theta_y \\ -\delta c\alpha\, \rho_y - \delta s\alpha\, \rho_x & -\delta s\alpha\, \rho_y + \delta c\alpha\, \rho_x & \delta\theta_y\, \rho_y + \delta\theta_x\, \rho_x \end{bmatrix} \tag{A-10}$$

and

$$(\Omega_{e/n}^n - \bar{\Omega}_{e/n}^n)\, C_g^n = \left(\begin{bmatrix} 0 & -\rho_z & \rho_y \\ \rho_z & 0 & -\rho_x \\ -\rho_y & \rho_x & 0 \end{bmatrix} - \begin{bmatrix} 0 & -\bar{\rho}_z & \bar{\rho}_y \\ \bar{\rho}_z & 0 & -\bar{\rho}_x \\ -\bar{\rho}_y & \bar{\rho}_x & 0 \end{bmatrix} \right) C_g^n$$

$$= \begin{bmatrix} 0 & \delta\rho_z & \rho_y - \bar{\rho}_y \\ -\delta\rho_z & 0 & -(\rho_x - \bar{\rho}_x) \\ -(\rho_y - \bar{\rho}_y) & \rho_x - \bar{\rho}_x & 0 \end{bmatrix} \begin{bmatrix} cos\alpha & sin\alpha & 0 \\ -sin\alpha & cos\alpha & 0 \\ 0 & 0 & 1 \end{bmatrix} \tag{A-11}$$

$$= \begin{bmatrix} -\delta\rho_z\, s\alpha & \delta\rho_z\, c\alpha & \rho_y - \bar{\rho}_y \\ -\delta\rho_z\, c\alpha & -\delta\rho_z\, s\alpha & -(\rho_x - \bar{\rho}_x) \\ -(\rho_e - \bar{\rho}_e) & \rho_n - \bar{\rho}_n & 0 \end{bmatrix}$$

For the wander azimuth frame transport rate vector is given in equation (4). The wander azimuth earth radii of curvature are approximated by a nominal value R. The velocity error in the wander azimuth frame is represented in the perturbation form and is given in equation (34). Substituting components of equation (34) into the corresponding elements in equation (4) yields for the transport rate errors

$$\rho_x - \bar{\rho}_x = -\frac{\delta v_y}{R} + \frac{v_y}{R^2}\, \delta h \tag{A-12}$$

$$\rho_y - \bar{\rho}_y = \frac{\delta v_x}{R} - \frac{v_x}{R^2}\, \delta h \tag{A-13}$$

where $\delta R \approx \delta h$.

The angular position dynamic error equations are obtained by equating elements in equations A-9, A-10 and A-11, and using equations A-12 and A-13. Equating the 1:3 elements in the E matrix equations, the following is obtained

$$\delta\dot{\theta}_y = -\rho_e\, \delta c\alpha + \rho_n\, \delta s\alpha - \frac{\delta v_x}{R} + \frac{v_x}{R^2}\, \delta h \tag{A-14}$$

Equating the 2:3 elements, the following is obtained

$$\delta\dot{\theta}_x = -\rho_e\, \delta s\alpha - \rho_n\, \delta c\alpha + \frac{\delta v_y}{R} - \frac{v_y}{R^2}\, \delta h \tag{A-15}$$

Attitude Error Dynamics

The "phi" form of the attitude error dynamics is [2]

$$\dot{\underline{\phi}} = \delta\underline{\rho} + \delta\underline{\omega}^n_{i/e} + \underline{\phi} \times \underline{\omega}^n_{i/n} + \underline{\epsilon}^n \qquad \text{A-16}$$

Using the correspondence in equation (18), the second term on the right side of this equation is expressed as

$$\begin{aligned}
\delta\underline{\omega}^n_{i/e} &= E\, C_n^g\, \underline{\omega}^n_{i/e} = E\, \underline{\omega}^g_{i/e} \\
&= \begin{bmatrix} \delta c\alpha & \delta s\alpha & -\delta\theta_y \\ -\delta s\alpha & \delta c\alpha & \delta\theta_x \\ \delta\theta_e & -\delta\theta_n & 0 \end{bmatrix} \begin{bmatrix} \Omega_n \\ 0 \\ \Omega_d \end{bmatrix} \\
&= \begin{bmatrix} \delta c\alpha\, \Omega_n - \delta\theta_y\, \Omega_d \\ -\delta s\alpha\, \Omega_n + \delta\theta_x\, \Omega_d \\ \Omega_n s\alpha\, \delta\theta_x + \Omega_n c\alpha\, \delta\theta_y \end{bmatrix} \qquad \text{A-17} \\
&= \begin{bmatrix} \delta c\alpha\, \Omega_n - \delta\theta_y\, \Omega_z \\ -\delta s\alpha\, \Omega_n + \delta\theta_x\, \Omega_z \\ -\Omega_y\, \delta\theta_x + \Omega_x\, \delta\theta_y \end{bmatrix}
\end{aligned}$$

Between the third and fourth lines $\delta\theta_e$ was obtained from equations A-2 and A-3, and the last line is obtained from

$$\underline{\Omega}^n = C_g^n\, \underline{\Omega}^g = \begin{bmatrix} c\alpha & s\alpha & 0 \\ -s\alpha & c\alpha & 0 \\ 0 & 0 & 1 \end{bmatrix} \begin{bmatrix} \Omega_n \\ 0 \\ \Omega_d \end{bmatrix} = \begin{bmatrix} \Omega_n c\alpha \\ -\Omega_n s\alpha \\ \Omega_d \end{bmatrix} \equiv \begin{bmatrix} \Omega_x \\ \Omega_y \\ \Omega_z \end{bmatrix} \qquad \text{A-18}$$

With the assumption that the z-tilt error is zero, $\phi_z \equiv 0$, the x and y components of the tilt error equation above become

$$\dot{\phi}_x = \frac{\delta v_y}{R} - \frac{v_y}{R^2}\delta h + \Omega_n\, \delta c\alpha - \Omega_z\, \delta\theta_y + \Omega_z\, \phi_y + \epsilon_x \qquad \text{A-19}$$

and

$$\dot{\phi}_y = -\frac{\delta v_x}{R} + \frac{v_x}{R^2}\delta h - \Omega_n\, \delta s\alpha + \Omega_z\, \delta\theta_x - \Omega_z\, \phi_x + \epsilon_y \qquad \text{A-20}$$

This assumption also implies

$$\dot{\phi}_z = 0 = \delta\rho_z - \Omega_y\, \delta\theta_x + \Omega_x\, \delta\theta_y + \omega_y\, \phi_x - \omega_x\, \phi_y + \epsilon_z$$

or

$$\delta\rho_z = \Omega_y\, \delta\theta_x - \Omega_x\, \delta\theta_y - \omega_y\, \phi_x + \omega_x\, \phi_y - \epsilon_z \qquad \text{A-21}$$

Velocity Error Dynamics

The perturbation form of the velocity error equation is [2]

$$\delta\dot{\underline{v}}^n = \underline{v}^n \times (\delta\underline{\omega}^n_{e/n} + 2\delta\underline{\omega}^n_{i/e}) - (\underline{\rho} + 2\underline{\Omega}) \times \delta\underline{v}^n + \underline{f}^n \times \underline{\phi} + \delta\underline{f}^n + \delta\underline{g}^n \qquad \text{A-22}$$

Errors in transport rate and earth rate were described above. The velocity erroor state components are presented in Figure 3.

APPENDIX B

Fine Alignment Error Equations

The coarse alignment Kalman filter estimates errors in the trigonometric functions $\delta\, s\alpha$ & $\delta\, c\alpha$ allowing for large errors in the wander azimuth angle. Below, the INS dynamic error model is modified to represent small angles.

The form for the wander angle error can be obtained from the developments in Appendix A. Equating the 1:1 elements for the E matrix equations results in the following

$$\begin{aligned}
\frac{d}{dt}(\delta c\alpha) &= \delta s\alpha\, \rho_d + \delta\theta_y\, \rho_e - \rho_z\, \delta s\alpha + \rho_y\, \delta\theta_e - \delta\rho_z\, s\alpha \\
&= \delta s\alpha\, (\rho_d - \rho_z) + \rho_e\, \delta\theta_y - \rho_y\, \delta\theta_e - \delta\rho_z\, s\alpha \qquad \text{B-1} \\
&= -\alpha\, \delta s\alpha + \rho_e\, \delta\theta_y - \rho_y\, \delta\theta_e - \delta\rho_z\, s\alpha
\end{aligned}$$

Substituting from equation A-21, and expressing the geographic frame referenced rate and position error terms as wander azimuth frame rates and position errors yields in the following

$$\begin{aligned}
\frac{d}{dt}(\delta c\alpha) &= -\alpha\, \delta s\alpha + \rho_e\, \delta\theta_y - \rho_y\, \delta\theta_e - \delta\rho_z\, s\alpha \\
&= -\alpha\, \delta s\alpha + (s\alpha\, \rho_x + c\alpha\, \rho_y)\, \delta\theta_y - \rho_y\, (s\alpha\, \delta\theta_x + c\alpha\, \delta\theta_y) \\
&\quad - (\Omega_y\, \delta\theta_x - \Omega_x\, \delta\theta_y - \omega_y\, \phi_x + \omega_x\, \phi_y - \epsilon_z)\, s\alpha \qquad \text{B-2} \\
&= -\alpha\, \delta s\alpha - s\alpha[(\rho_y + \Omega_y)\delta\theta_x - (\rho_x + \Omega_x)\delta\theta_y - \omega_y\phi_x + \omega_x\phi_y - \epsilon_z] \\
&= -\alpha\, \delta s\alpha - s\alpha[\omega_y\delta\theta_x - \omega_x\delta\theta_y - \omega_y\phi_x + \omega_x\phi_y - \epsilon_z]
\end{aligned}$$

From equation (20), the left hand side of equation B-2 is also equivalent to

$$\begin{aligned}
\frac{d}{dt}(\delta c\alpha) &= -\left(\frac{d}{dt} s\alpha\right) \delta\alpha - s\alpha \left(\frac{d}{dt}\delta\alpha\right) \\
&= -c\alpha\, \alpha\, \delta\alpha - s\alpha \left(\frac{d}{dt}\delta\alpha\right) \qquad \text{B-3} \\
&= -\alpha\, \delta s\alpha - s\alpha \left(\frac{d}{dt}\delta\alpha\right)
\end{aligned}$$

Equating the corresponding terms in equations B-2 and B-3, the following equation for wander azimuth angle error is obtained

$$\frac{d}{dt}(\delta\alpha) = \omega_y\, \delta\theta_x - \omega_x\, \delta\theta_y - \omega_y\, \phi_x + \omega_x\, \phi_y - \epsilon_z \qquad \text{B-4}$$

The INS system error dynamic model for small error angles can be obtained from the developments in Appendix A. Using equations (19) and (20), the y component of position error from equation A-14 becomes

$$\begin{aligned}
\delta\dot{\theta}_y &= -\rho_e\, \delta c\alpha + \rho_n\, \delta s\alpha - \frac{\delta v_x}{R} + \frac{v_x}{R^2}\delta h \\
&= -\rho_e\, (-s\alpha\, \delta\alpha) + \rho_n\, (c\alpha\, \delta\alpha) - \frac{\delta v_x}{R} + \frac{v_x}{R^2}\delta h \qquad \text{B-5} \\
&= (\rho_n\, c\alpha + \rho_e\, s\alpha)\, \delta\alpha - \frac{\delta v_x}{R} + \frac{v_x}{R^2}\delta h \\
&= \rho_x\, \delta\alpha - \frac{\delta v_x}{R} + \frac{v_x}{R^2}\delta h
\end{aligned}$$

The x component of position is obtained similarly. The velocity and tilt error equations can be obtained using the following

$$\Omega_n\, \delta c\alpha = \Omega_y\, \delta\alpha \quad \& \quad \Omega_n\, \delta s\alpha = \Omega_x\, \delta\alpha \qquad \text{B-6}$$

Substituting these expressions into equations for the velocity and attitude errors in Appendix A yields the model in Figure 4.